# CAPTURING MATHEMATICAL AND HUMAN PERCEPTIONS OF SHAPE AND FORM THROUGH MACHINE LEARNING

**Gopsill, James (1,2);**
**Goudswaard, Mark (1);**
**Jones, David (1);**
**Hicks, Ben (1)**

1: Design Manufacturing Futures Lab, School of Civil, Aerospace and Mechanical Engineering, University of Bristol, UK;
2: Centre for Modelling and Simulation, Bristol, UK

## ABSTRACT

Classifying shape and form is a core feature of Engineering Design and one that we do this instinctively on a daily basis. Matching similar components to then reduce unique component counts, determining whether a competitors design infringes on copyright and receiving market feedback on product styling are all examples where shape and form comes into play. However, shape and form can be perceived in different ways from purely mathematical (e.g. shape grammars) to wholly subjective (e.g. market feedback) and these perceptions may not entirely agree.
This paper examines the mathematical and human perceptions of shape and form through a study of classifying shapes that have been interpolated between one another, and in doing so, highlights the disparity in perceptions. Following this, the paper demonstrates how the emergent field of Machine Learning can be applied to capture mathematical and human perceptions of shape and form resulting in a means to twin this feedback into product development.

**Keywords**: Machine learning, Evaluation, User centred design, shape and form, perception

**Contact**:
Gopsill, James
University of Bristol
Mechanical Engineering
United Kingdom
james.gopsill@bristol.ac.uk

**Cite this article:** Gopsill, J., Goudswaard, M., Jones, D., Hicks, B. (2021) 'Capturing Mathematical and Human Perceptions of Shape and Form Through Machine Learning', in *Proceedings of the International Conference on Engineering Design (ICED21),* Gothenburg, Sweden, 16-20 August 2021. DOI:10.1017/pds.2021.59

# 1 INTRODUCTION

Classifying shape and form is a core feature of Engineering Design. Examples include component matching, determining whether a competitors' design infringes on copyright, receiving market feedback on product styling, and conformance to implicit rule sets (e.g., a chess piece conforming to the rules that would classify it as a pawn or a set of chess pieces conforming to the rules of being a self-consistent set). The emergence of Machine Learning (ML) provides new opportunities in how we capture and classify shape and form. These methods train on pre-classified datasets and use this understanding to classify new data with varying degrees of confidence. Many are trained on images which can be advantageous as it removes the need to develop algorithms that can post-process shape and form data for fitting mathematical descriptors. It may also be a useful substitute where a mathematical descriptor does not exist, and it is either too challenging or too costly to develop. For example, automotive companies will have mathematical descriptors of the shape and form of their cars to ensure future design iterations conform to brand and image (Burnap et al., 2016). However, these will be closely guarded trade secrets. Thus, there is an opportunity to use ML to represent the underlying descriptors of brands to assist companies in ensuring their designs are not perceived as a competitors' design.

One can also consider the algorithm viewing an image as analogous to a human viewing an image. Thus, there may be the potential for ML to represent human perception of shape and form. If true, this could have a significant impact for designs that are highly dependent on customer feedback as they could be replaced by ML trained on a target market customer-base. The result would lead to twinned[1] 'customer' feedback throughout the design process as renders/photos of a products shape and form – as it is being developed – could be analysed via ML.

As shape and form can be perceived in different ways ranging from purely mathematical (e.g., shape grammars) to wholly subjective (e.g., market feedback), research into whether ML can capture the range of perception is required. Figure 1 illustrates this by showing a square transforming to a circle. The mathematical function used[2] would define the transition point between classifications as (5). But would a human perceive it as (5)? At what point do you think the square becomes a circle? And would your colleagues select the same point? If not, then what is the variation of perception across society? While a seemingly trivial example, understanding this is crucial in being able to support the aforementioned shape and form classification activities. Having this understanding will also ensure that we apply the right training set to an ML for a given shape and form design activity.

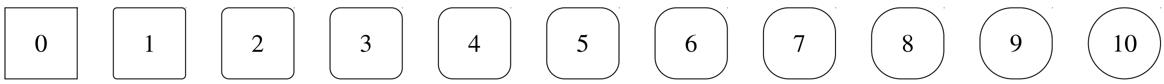


*Figure 1. Square or circle? When do you feel the shape has transitioned from a square to a circle?*

These concepts have driven the paper's contribution in further understanding mathematical and human perceptions on shape and form, and whether ML can be used to represent them. The contribution is also positioned toward design science rather than design practice. The paper continues by discussing the related work in classifying shape and form, and how they have been applied in Engineering Design (Section 2). A description of the experiment used to evaluate mathematical and human perceptions on shape classification and ML's ability to capture them is then provided (Section 3). The results are subsequently presented (Section 4) followed by a discussion with regards to the opportunities to pull this research through to design practice, implications to design research and future areas of work (Section 5). The paper then concludes highlighting the key findings from the study (Section 6).

# 2 RELATED WORK

To situate the work, a brief overview of related work in the mathematical and human perception of shape and form, and ML in Engineering Design is provided.

---

1 Real-time synchronisation of data and information.
2 An edge rounding function commonly found in Computer Aided Design programs.


https://doi.org/10.1017/pds.2021.59 Published online by Cambridge University Press

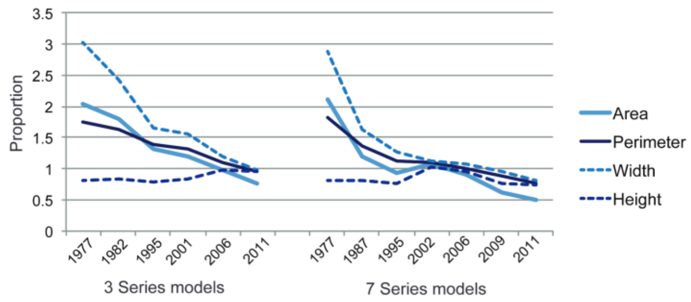


*(a) Convergence on brand identity over time (Ranscombe et al., 2012a).*

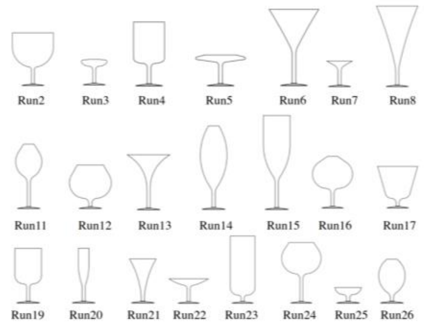


*(b) Twinning wine glass form with market feedback to generate the optimal form (Kittidecha and Marasinghe, 2015).*

*Figure 2. Mathematical perceptions on design.*

## 2.1 Mathematical perceptions on shape and form

Mathematical descriptors of shape and form has extant research that cannot be done justice in a few paragraphs. Here, we detail some examples of how mathematical descriptors have been used to evaluate shape and form in the context of Engineering Design.

Ranscombe et al., (2012a,b) identified headlights as a key feature for automotive vehicle branding with consumers able to differentiate between vehicles based on this feature more so than the overall form of the vehicle. Their work demonstrated how human perceptions can be explained mathematically. Subsequent analysis of headlight silhouettes through the application of path descriptors[3] revealed vehicles from different brands feature a distinct set of coefficients with each generation of vehicle only ever slightly perturbing them (Figure 2a). They propose that there is a maximum acceptable perturbation of form from one vehicle to the next to maintain to ensure consistent branding across a product portfolio.

Kittidecha and Marasinghe, (2015) twinned a Box–Behnken response surface parametric design that used customer feedback to explore the design space of a wine glass. The feedback was used to directly manipulate the parametric design and an iterative design process led to solution convergence for the target market (Figure 2b). Wine glass form has also been investigated by Venturi et al., (2016) who show a coupled perception of wine glass and wine quality. Achieving these feedback mechanisms enables designers to optimise their designs for a target market in a greatly reduced time thereby enabling businesses to react quickly to consumer trends.

## 2.2 Human perception on shape and form

Human perception of shape and form has been of interest to designers and the arts. Graphic artist M. C. Escher is famous for his work on manipulating shape and form through his mathematically inspired woodcuts and lithographs. An example of this is Metamorphosis II – a thirteen feet long woodcut strip (Escher, 1989). A portion of this is shown in Figure 3 where subsequent transformations of lizards to hexagons to honeycombs to bees are depicted. Escher's work demonstrates how form can be transformed drastically yet seamlessly.

Achieving these brilliant transformations in the first half of the 20th century required years of practice and a good helping of natural talent. Today, we are fortunate to have tools that can assist us in generating these transforms. However, to make them seamless it is necessary to understand the human perception of these transformations.

## 2.3 Machine Learning

The application of ML in Engineering Design is a rapidly emerging field of inquiry with the potential to impact many activities. For example, Zaki et al., (2016) trained a Convolutional Neural Network (CNN) on multi-view renders of 3D geometry and used the resulting CNN to classify other 3D

[3] Length, enclosed area and Fourier series.



https://doi.org/10.1017/pds.2021.59 Published online by Cambridge University Press

geometry. A potential design practice application of the method is the matching of similar parts across product families with a view to reduce part variety in an organisations' supply chain.

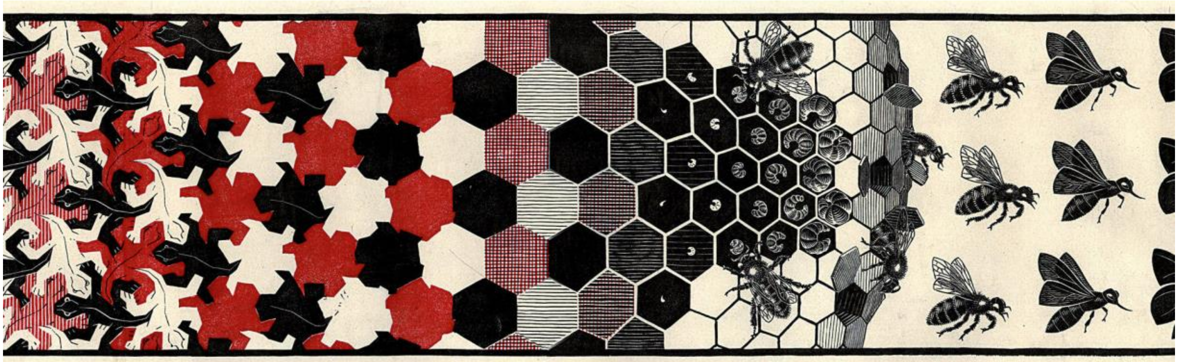

*Figure 3. Metamorphosis II (Escher, 1989).*

Maturana and Scherer, (2015) augmented depth mapped images with Neural Networks to develop voxel-based approximations of objects within a scene enabling rapid scene object detection. This could impact design practice in providing a means to describe the locations that products are deployed and used in.

Gopsill and Jennings, (2020) used a CNN as an information search and retrieval tool for large model repositories, such as Thingiverse and GrabCAD, to enable the democratisation of design. The CNN enables users to take a photo of the item that they wish to print with the CNN returning the closest matching results in the repository. The result is users do not need to describe the shape, form or type of an object where language and lexicons can become a barrier. ML as an information search and retrieval tool has also been evidenced by Real et al., (2021) who revealed that as one increases the number of model classifications ($\geq$ 1000), the CNN's accuracy for an exact match – suitable for twinning – diminished but it's top-10 ranking would often include a suitably matched model.

The examples provided here show that the application of ML in Engineering Design is still exploratory and at the design science stage. This is essential as this work will form the underlying tools that design practice researchers can pull through, develop and apply to real-world Engineering Design problems.

### 2.4 Summary

In summary, the perception of shape and form has research in both mathematical and human domains and is extensively observed in Engineering Design. Challenges lie in how the two can be used together and in understanding how they compare with one another when evaluating shape and form. ML's traction in Engineering Design is increasing and is already being applied to both real and rendered images that inherently capture the shape and form of the products we make. ML in Engineering Design is still in its early phases and requires further founding work that design practitioners and practice researchers can pull through and apply the ideas to real-world engineering problems. Therefore, this paper situates itself as the bridge between the perceptions of shape and form, and application of ML by exploring whether ML could be trained to capture both mathematical and human perceptions of shape and form.

## 3 EXPERIMENT. PERCEPTIONS OF 2D GEOMETRIC PRIMITIVES

The experiment's objectives were threefold. First, compare mathematical and human perceptions of shape and form. Second, characterise the variance in human perception. Third, elucidate whether CNNs can be trained to replicate both mathematical and human perception. To achieve this, the experiment involved the:

1. curation of a shape dataset;
2. generation of a survey to capture user perception;
3. analysis of the survey results; and,
4. training and validation of CNNs using mathematical and human perception data.

These are expanded upon in the subsequent sections.


https://doi.org/10.1017/pds.2021.59 Published online by Cambridge University Press

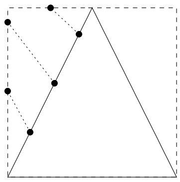

*Figure 4. Example interpolation between a triangle and square.*

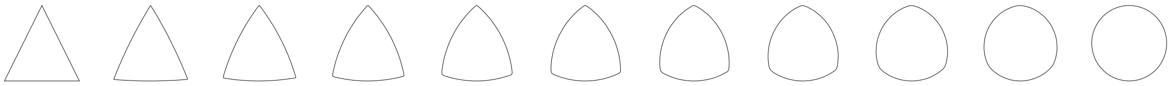

*(a) Triangle to circle.*

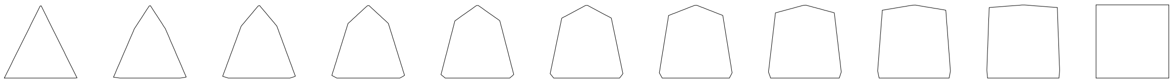

*(b) Triangle to square.*

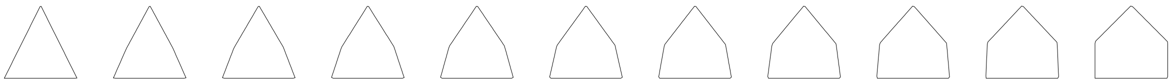

*(c)Triangle to pentagon.*

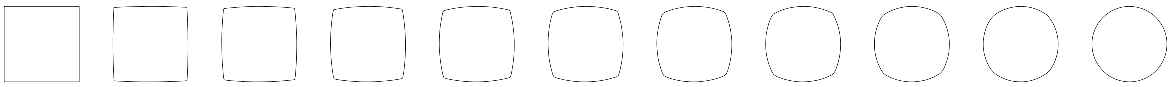

*(d) Square to Circle.*

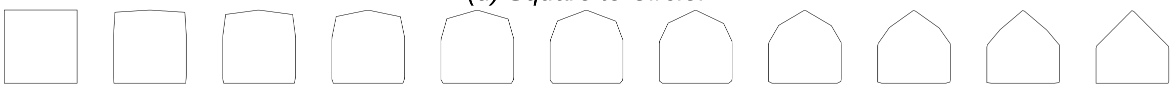

*(e) Square to pentagon.*

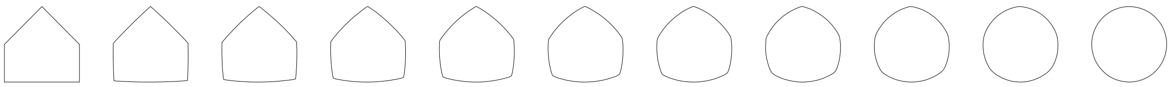

*(f) Pentagon to circle.*

*Figure 5. 2D shapes.*

### 3.1 Shape curation

The experiment necessitates a library of shapes and a set of underlying functions that can interpolate between them. To achieve this, the study utilised two javascript shape libraries that are used for 2D graphics – Paper.js[4] and Flubber.js[5]. Paper.js provided the means to create the initial shape paths and control the number of points used to represent them. These were then fed into Flubber.js that features an interpolation algorithm to transform one shape to another, thus forming our shape grammar (Figure 4). A constant number of points (100) was used to describe each shape to ensure consistency in the interpolation. 2D primitives, Circle, Pentagon, Square and Triangle, were selected as these form the fundamental building blocks for many Computer Aided Engineering operations. Examples, include Computer-Aided Design (CAD), sketching, illustration, presentation and word processing applications. Majoral et al., (2018) study into Spatial Augmented Reality (SAR) to support industrial design revealed industrial designers still wished for the inclusion of 2D primitive geometry as it is still essential to their practice.

The primitives also present in early-years education. This acts as a control by reducing the potential misunderstanding in the descriptions required for the shape classification problem. The shapes were interpolated at 10% intervals resulting in the dataset of shapes shown in Figure 5. Code to generate these shapes is provided in the accompanying data repository and can be found at http://data.bris.ac.uk.

[4] J. Lehni and J. Puckey, https://github.com/paperjs/paper.js, visited: 2020-03-03.
[5] N. Veltman, https://github.com/veltman/flubber, visited: 2020-03-03.



https://doi.org/10.1017/pds.2021.59 Published online by Cambridge University Press

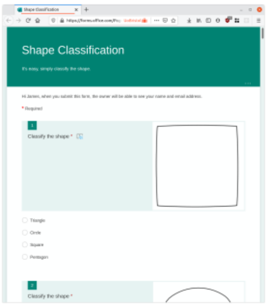


(a) *Microsoft Forms Survey.*

| $\kappa$ | Level of Agreement |
|---|---|
| $< 0$ | Poor |
| 0.01 – 0.20 | Slight |
| 0.21 – 0.40 | Fair |
| 0.41 – 0.60 | Moderate |
| 0.61 – 0.80 | Substantial |
| 0.81 – 1.00 | Almost Perfect |

(b) *Interpretation of $\kappa$ (Landis and Koch, 1977).*

*Figure 6. Survey.*

## 3.2 Survey

Each shape transform was taken and placed into a survey for participants to complete (Figure 6). The survey consisted of 58 questions, one mapping to each shape from Figure 5, and the task for the participant was to classify each one as either a Triangle, Circle, Square or Pentagon. Shapes were provided to participants out of context (i.e., not in the sequence of the transform) in order to reduce bias based on previous shape classifications. Shapes were also ordered randomly for each participant.

## 3.3 Evaluation

The data from the survey was evaluated with respect to the difference in the mathematical and human perceptions and variance in human perception. Mathematical perception was defined as the mid-point between two geometric entities.

Human perception was defined using inter-coder reliability across the participants' classification responses (Fleiss and Cohen, 1973). The results from the survey were collated to produce a matrix, $M$, of $m$ shapes6, $s$, as the row vector and their summed classification7 scores, $c$, as the column vector (Equation (1)).

$$M = \begin{array}{c} \\ s_1 \\ s_2 \\ s_3 \\ \vdots \\ s_m \\ p_j \end{array} \begin{array}{c} \begin{array}{ccccc} c_1 & c_2 & \cdots & c_n \end{array} \\ \begin{pmatrix} 0 & 5 & \cdots & 0 \\ 1 & 0 & \cdots & 1 \\ 0 & 2 & \cdots & 1 \\ \vdots & \vdots & \ddots & \vdots \\ 0 & 3 & \cdots & 1 \end{pmatrix} \\ \begin{array}{ccccc} p_1 & p_2 & \cdots & p_n \end{array} \end{array} \begin{array}{c} P_i \\ P_1 \\ P_2 \\ P_3 \\ \vdots \\ P_m \\ \\ \end{array} \tag{1}$$

With $M$, we apply Fleiss' kappa, $\kappa$, which provides the reliability of agreement between the $N$ coders. To start, we calculate the level of agreement between the coder on the i-th shape, $P_i$, and calculate the proportion of assignments to the j-th classification, $p_j$ .

$$P_i = \frac{1}{n(n-1)} \sum_{j=1}^{k} n_{ij}(n_{ij} - 1),\ p_j = \frac{1}{Nn} \sum_{i=1}^{N} n_{ij} \tag{2}$$

With these, we can calculate Fleiss' kappa:

$$\kappa = \frac{\bar{P} - \bar{P}_e}{1 - \bar{P}_e} \text{ where } \bar{P} = \frac{1}{N} \sum_{i=1}^{N} P_i\ ,\ \bar{P}_e = \sum_{j=1}^{k} p_j^2 \tag{3}$$

Having calculated $\kappa$, we refer to Figure 6b to interpret the level of agreement attained.

The matrices (Equation (1)) also provide an indication of where and when participants transition from one shape to another and if there are any other shape classifications involved during the transition. By analysing the delta between classifications during a transition, we can determine the median transition

6 $m$ = 58 and are the shapes shown in Figure 5.
7 $n$ = 4 and are Circle, Triangle, Square or Pentagon.


https://doi.org/10.1017/pds.2021.59 Published online by Cambridge University Press

point for the population. This can then be compared to the mathematical model that denotes the transitions as halfway through the transformation.

*Table 1. CNN mathematical procedure parameter values.*

| Parameter | Value | Parameter | Value |
|---|---|---|---|
| Image Size | 228x228 | Batch Size | 3 |
| Training: Validation Split | 80:20 | Convolution Layers | 1 to 3 (default 3) |
| Kernel Size | 3 to 5 | Activation | Rectified Linear Unit (ReLU) |
| Optimiser | adam, sgd (choice between) | Loss | Categorical Cross-Entropy |
| Metrics | Accuracy | Early Stopping Monitor | Value loss |
| Early Stopping Patients | 10 | Learning Rate Reduction Patients | 2 |
| Learning Rate Reduction Factor | 0.5 | Minimum Learning Rate | 0.00001 |
| Hyperband Objective | Value Accuracy | Hyperband Max Epochs | 200 |
| Hyperband Executions per Trial | 3 | Tuner Search Epochs | 20 |
| Tuner Search Callbacks | Early Stopping, Learning Rate Reduction | Model Fitting Epochs | 200 |
| Model Fitting Callbacks | Early Stopping, Learning Rate Reduction | | |

### 3.4 Training and validating a CNN on mathematical and user perception

Training and validation of the CNN used the open-source ML Python libraries TensorFlow (Abadi et al., 2016) and Keras Tuner[8]. Keras Tuner and Tensorflow work in tandem to generate, train and test CNN architectures. The objective of the tuner is to search for an optimal architecture for a given data set within a predefined set of conditions. The tuner was set to use the Hyperband approach (Li et al., 2017). The Hyperband approach was configured for validation accuracy and bounded by a max epoch of 200, 1 to 3 convolution layers, an early stopping clause to prevent over fitting, and adjusted learning rates as the search neared an optimal solution. The tuner workflow loaded the data sets with an 80/20 training/validation split and used Hyperband optimisation to search for an optimal set of hyperparameters before fitting the CNN architecture to the data set. A full list of tuner variables and their respective settings is presented in Table 1. The process is further detailed in a Jupyter Notebook stored in the accompanying data repository – http://data.bris.ac.uk.
The process was performed on a cloud-based virtual machine hosted by PaperSpace[9]. PaperSpace provide a ‘ML-in-a-box’ package tailored specifically to ML applications. This package consists of Ubuntu 18.04 LTS with a Python 3.6 environment pre-configured with the ML libraries. The GPU used to train the model was a NVIDIA Quadro P4000 GPU with 8GB GDDR5 RAM and 1,792 CUDA cores. The process was used to train and validate CNN models for three perception data sets:

- **Mathematical**. A training set produced from the mathematical transform with the images classified based on the 0.5 interpolation boundary.
- **Human most popular**. The most popular vote for each of the 58 shapes in the survey being used to classify the shape.
- **Human votes**. The shapes were classified according to raw survey results. Where participants had classified the shape the same, a duplicate image was placed in the training set. Thus, the training set becomes a function of participants ($58N$).

## 4 RESULTS

The user perception classification and inter-coder reliability scores are shown in Tables 2 and 3, respectively. The CNN results are shown in Figure 7. Table 2 highlights a strong agreement (0.763) between coders across the shape transformations. Table 3 provides a more detailed comparison of the variance between coders. Grey columns indicate the two shapes the transform was moving between. Grey rows indicate the period of uncertainty between coders and the values at which the coders transitioned from one shape classification to another. Figure 7 provides the overall accuracy score based on the 80/20 train/validation regime and the resulting confusion matrices from those tests.

[8] Keras, https://keras-team.github.io/keras-tuner/, visited: 2020-12-03.
[9] Paperspace, https://www.paperspace.com/, visited: 2020-12-03


https://doi.org/10.1017/pds.2021.59 Published online by Cambridge University Press

*Table 2. User perception agreement, $\kappa$. The inter-coder reliability reveals a strong agreement across participants in being able to code the 2D primitives.*

| Statistic | Value |
|---|---|
| $\sum_{i=1}^{n} P_i$ | 39.667 |
| $\bar{P}$ | 0.826 |
| $\bar{P}_e$ | 0.267 |
| $\kappa$ (Strong Agreement) | 0.763 |

*Table 3. User perception classification results (T = Triangle, C = Circle, S = Square and P = Pentagon). Grey columns indicate the two shapes involved in the transformation. Grey rows indicate the period of uncertainty between coders in classifying the shape.*

Triangle to Circle

| Shape Transition | Classification T | S | C | P | $P$ |
|---|---|---|---|---|---|
| T | 12 | 0 | 0 | 0 | 1.00 |
| 0.1 | 12 | 0 | 0 | 0 | 1.00 |
| 0.2 | 12 | 0 | 0 | 0 | 1.00 |
| 0.3 | 12 | 0 | 0 | 0 | 1.00 |
| 0.4 | 12 | 0 | 0 | 0 | 1.00 |
| 0.5 | 12 | 0 | 0 | 0 | 1.00 |
| 0.6 | 12 | 0 | 0 | 0 | 1.00 |
| 0.7 | 10 | 0 | 2 | 0 | 0.70 |
| 0.8 | 3 | 0 | 9 | 0 | 0.59 |
| 0.9 | 0 | 0 | 12 | 0 | 1.00 |
| C | 0 | 0 | 12 | 0 | 1.00 |

Triangle to Square

| Shape Transition | Classification T | S | C | P | $P$ |
|---|---|---|---|---|---|
| T | 12 | 0 | 0 | 0 | 1.00 |
| 0.1 | 12 | 0 | 0 | 0 | 1.00 |
| 0.2 | 9 | 0 | 0 | 3 | 0.59 |
| 0.3 | 4 | 0 | 0 | 8 | 0.52 |
| 0.4 | 3 | 0 | 0 | 9 | 0.59 |
| 0.5 | 2 | 0 | 0 | 10 | 0.70 |
| 0.6 | 1 | 1 | 0 | 10 | 0.68 |
| 0.7 | 1 | 5 | 0 | 6 | 0.38 |
| 0.8 | 0 | 9 | 0 | 3 | 0.59 |
| 0.9 | 0 | 11 | 0 | 1 | 0.83 |
| S | 0 | 12 | 0 | 0 | 1.00 |

Square to Circle

| Shape Transition | Classification T | S | C | P | $P$ |
|---|---|---|---|---|---|
| S | 0 | 12 | 0 | 0 | 1.00 |
| 0.1 | 0 | 12 | 0 | 0 | 1.00 |
| 0.2 | 0 | 12 | 0 | 0 | 1.00 |
| 0.3 | 0 | 11 | 1 | 0 | 0.83 |
| 0.4 | 0 | 12 | 0 | 0 | 1.00 |
| 0.5 | 0 | 12 | 0 | 0 | 1.00 |
| 0.6 | 0 | 12 | 0 | 0 | 1.00 |
| 0.7 | 0 | 2 | 10 | 0 | 0.70 |
| 0.8 | 0 | 0 | 12 | 0 | 1.00 |
| 0.9 | 0 | 0 | 12 | 0 | 1.00 |
| C | 0 | 0 | 12 | 0 | 1.00 |

Square to Pentagon

| Shape Transition | Classification T | S | C | P | $P$ |
|---|---|---|---|---|---|
| S | 0 | 12 | 0 | 0 | 1.00 |
| 0.1 | 0 | 12 | 0 | 0 | 1.00 |
| 0.2 | 0 | 12 | 0 | 0 | 1.00 |
| 0.3 | 0 | 9 | 0 | 3 | 0.59 |
| 0.4 | 0 | 8 | 0 | 4 | 0.52 |
| 0.5 | 0 | 7 | 0 | 5 | 0.47 |
| 0.6 | 1 | 4 | 0 | 7 | 0.41 |
| 0.7 | 1 | 1 | 0 | 10 | 0.68 |
| 0.8 | 1 | 0 | 0 | 11 | 0.83 |
| 0.9 | 1 | 0 | 0 | 11 | 0.83 |
| P | 1 | 0 | 0 | 11 | 0.83 |

Pentagon to Circle

| Shape Transition | Classification T | S | C | P | $P$ |
|---|---|---|---|---|---|
| P | 1 | 0 | 0 | 11 | 0.83 |
| 0.1 | 1 | 1 | 0 | 10 | 0.68 |
| 0.2 | 1 | 0 | 0 | 11 | 0.83 |
| 0.3 | 0 | 0 | 0 | 12 | 1.00 |
| 0.4 | 0 | 0 | 0 | 12 | 1.00 |
| 0.5 | 0 | 0 | 0 | 12 | 1.00 |
| 0.6 | 0 | 0 | 0 | 12 | 1.00 |
| 0.7 | 0 | 0 | 6 | 6 | 0.45 |
| 0.8 | 0 | 0 | 11 | 1 | 0.83 |
| 0.9 | 0 | 0 | 12 | 0 | 1.00 |
| C | 0 | 0 | 12 | 0 | 1.00 |

## 4.1 Difference and variance in mathematical and user perception

Table 3 reveals coders rarely transitioned between shapes at the 0.5 mark as the mathematical definition describes. In particular, if we look at the transitions from Triangle/Square/Pentagon to Circle, the transition point is closer to 0.7. This indicates humans perceive a Circle in a different sense to that of other shapes.

It is as if a Circle is less accommodating to variations of its form compared to other shapes. In addition, the consistency at which the participants decided that the shape is now a Circle denotes there is a clear transitional boundary independent of the shape it is being interpolated from. The results confirm humans do perceive shapes differently to the mathematical perception.

If we take a look at the transitions between other shapes, the boundaries appear less ‘fixed’ compared to the Circle with greater variance being exhibited. Both Triangle to Square and Square to Pentagon featured a large variance across coders with the transition ranging between 0.2–0.8 with participants steadily transitioning across this period. Triangle to Square also featured variance with participants classifying the interpolated shape as a Pentagon. This is interesting as the mathematical description does not account for the possibility of the interpolation being classified as a shape other than its two constituent parts.

## 4.2 CNNs trained on mathematical and human perceptions

An optimal architecture was achieved within 50 of the 200 epochs for all three CNNs. The architectures are described in Table 4 and it can be seen that there is little variance in the number and type of layer employed. The main difference observed is the tuner selecting between max and average pooling. This indicates that the architecture is closely coupled with the input data type rather than the classification leading to little change being required to optimally represent mathematical and human perceptions. It also shows that the same architecture could perform well for representing both mathematical and human perceptions.

Figure 7 shows the confusion matrices for the three CNNs. The CNN trained on the Mathematical shape classifications resulted in a 75% accurate replication of the mathematical function. Thus, it shows promise that an ML could be used to reverse-engineer the mathematical descriptor of a set of shapes. The CNN trained on the Human Most Popular dataset produced a 70% accurate result in determining the shape classification (Figure 7b). This is also promising as the agreement between humans was 76% so the ‘error’ in the CNN classification is in line with the inter-coder reliability of the participants. Thus, one could consider the ML as representative of a human coder. If we include the weightings as per the Human Voted Dataset, we achieve a 79.5% accurate result in predicting the popular voted classification (Figure 7c). Thus, we can also train the CNN to provide the population view.



https://doi.org/10.1017/pds.2021.59 Published online by Cambridge University Press

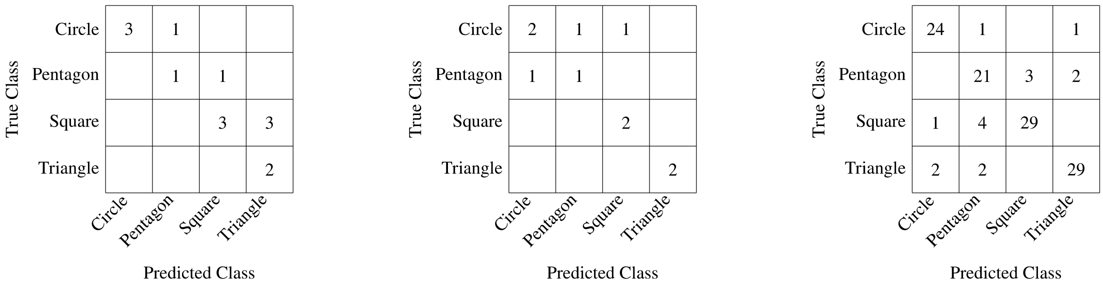


(a) Mathematical (75%). (b) Most popular (70%). (c) Votes (79.5%)

*Figure 7. Confusion matrices for the CNNs showing with overall accuracy noted in the sub-captions.*

*Table 4. CNN architectures to capture human and mathematical perceptions of shape and form.*

| Mathematical | | | Most Popular | | | Votes | | |
|---|---|---|---|---|---|---|---|---|
| Layer (type) | Output Shape | Var # | Layer (type) | Output Shape | Var # | Layer (type) | Output Shape | Var # |
| input_1 (InputLayer) | [(228, 228, 3)] | 0 | input_1 (InputLayer) | [(228, 228, 3)] | 0 | input_1 (InputLayer) | [(228, 228, 3)] | 0 |
| conv2d | (228, 228, 12) | 588 | conv2d | (228, 228, 8) | 392 | conv2d | (228, 228, 20) | 560 |
| max_pooling2d | (114, 114, 12) | 0 | average_pooling2d | (114, 114, 8) | 0 | average_pooling2d | (114, 114, 20) | 0 |
| batch_normalization | (114, 114, 12) | 48 | batch_normalization | (114, 114, 8) | 32 | batch_normalization | (114, 114, 20) | 80 |
| re_lu | (114, 114, 12) | 0 | re_lu | (114, 114, 8) | 0 | re_lu | (114, 114, 20) | 0 |
| conv2d_1 | (114, 114, 16) | 1744 | conv2d_1 | (114, 114, 16) | 1168 | conv2d_1 | (114, 114, 16) | 2896 |
| max_pooling2d_1 | (57, 57, 16) | 0 | max_pooling2d | (57, 57, 16) | 0 | max_pooling2d | (57, 57, 16) | 0 |
| batch_normalization_1 | (57, 57, 16) | 64 | batch_normalization_1 | (57, 57, 16) | 64 | batch_normalization_1 | (57, 57, 16) | 64 |
| re_lu_1 | (57, 57, 16) | 0 | re_lu_1 | (57, 57, 16) | 0 | re_lu_1 | (57, 57, 16) | 0 |
| conv2d_2 | (57, 57, 28) | 7196 | conv2d_2 | (57, 57, 16) | 6416 | conv2d_2 | (57, 57, 20) | 8020 |
| max_pooling2d_2 | (28, 28, 28) | 0 | average_pooling2d_1 | (28, 28, 16) | 0 | max_pooling2d_1 | (28, 28, 20) | 0 |
| batch_normalization_2 | (28, 28, 28) | 112 | batch_normalization_2 | (28, 28, 16) | 64 | batch_normalization_2 | (28, 28, 20) | 80 |
| re_lu_2 | (28, 28, 28) | 0 | re_lu_2 | (28, 28, 16) | 0 | re_lu_2 | (28, 28, 20) | 0 |
| global_max_pooling2d | (28) | 0 | global_max_pooling2d | (16) | 0 | global_max_pooling2d | (20) | 0 |
| dense | (4) | 116 | dense (Dense) | (4) | 68 | dense (Dense) | (4) | 84 |

## 5 DISCUSSION

The study has revealed that differences exist between mathematical and human perceptions of shape and form. Whilst mathematical perceptions can provide uniform and even descriptions of shapes, human perceptions reveal that definitions of certain shapes have significantly stricter boundary definitions than others. For example, human perception of the Circle transition point occurs much later in the transformation path, while the Pentagon featured more widely and across many transformations. This is an interesting finding that could have a significant impact in how we perceive brand design/IP infringements as there may be particular features that humans will claim has highly bounded (e.g., a circle) while others are amorphous. It also highlights that a mathematical comparison is unlikely to represent the human perception of shape and form, and poses an interesting question as to which society uses for brand identity/design copyright infringements.

The results also show that CNNs are a promising technique for capturing mathematical and human perceptions of shape and form. This paper has shown that CNNs are able to represent the mathematical descriptor of a shape classifier. This has significant potential as CNNs could be used by engineering designers to capture rule-sets inherent in designed products, for example, rules that dictate a chess piece being of a specific type, as well as analysing what makes a brand identifiable and distinguishable from other brands. The paper has also demonstrated that CNNs are able to represent human perception, both at an individual and population level.

However, further work is required to evaluate the extent at which CNNs can capture the various mathematical interpretations that exist as well as evaluate human perceptions on a greater variety of shapes and form. One route to expand the study would be through crowd sourcing platforms, such as Amazon Mechanical Turk, to receive a much greater response sample size to the survey. Improvements to the survey methodology could be made where the participants would have to first classify the non-interpolated shapes before being shown the interpolated shapes in a random order. This control would ensure that participants are able to distinguish between the fundamental shapes ahead of classifying the subsequent transformations. Having demonstrated the ability to capture both mathematical and human perceptions of shape and form, there now exists the opportunity to develop the capability further and


https://doi.org/10.1017/pds.2021.59 Published online by Cambridge University Press

study how it can be introduced into the design process. Application areas include: (1) informing a designer as they work on a CAD model; (2) incorporating the results in the feedback loop of generative design processes; and/or, (3) using the CNN to map the design space of a parametric model.

## 6 CONCLUSION

Classifying shape and form is a core feature of Engineering Design and can be perceived both objectively and subjectively. This paper confirms that mathematical and human perceptions are not equivalent and that it is therefore important to use the appropriate perception when designing products. The paper has also shown Machine Learning has the capability to replicate mathematical and human perceptions of shape and form. This could transform design through the ability to assist designers in conforming to inherent design rules, such as brand identity, and to receive twinned ‘customer’ feedback through a ML trained on human perception. Having this feedback in near real-time and throughout the design process could reduce product development cycles and support right first-time products for consumer markets.

## ACKNOWLEDGEMENTS

The work has been undertaken as part of the Engineering and Physical Sciences Research Council (EPSRC) grants – EP/R032696/1 and EP/V05113X/1. The authors would like to also thank the University of Bristol and Centre for Modelling and Simulation in supporting this research, PaperSpace for the ‘ML-in-a-box’ solution, and the creators of open-source tools.

## REFERENCES

Abadi, M., Agarwal, A., Barham, P., Brevdo, et al., 2016. Tensorflow: large-scale machine learning on heterogeneous distributed systems. Arxiv preprint arxiv:1603.04467.

Burnap, A., Hartley, J., Pan, Y., Gonzalez, R., and Papalambros, P.Y., 2016. Balancing design freedom and brand recognition in the evolution of automotive brand styling. Design science, 2, e9.

Escher, M., 1989. Escher on Escher: Exploring the infinite. Abrams.

Fleiss, J.L. and Cohen, J., 1973. The equivalence of weighted kappa and the intraclass correlation coefficient as measures of reliability. Educational and psychological measurement, 33(3), pp.613–619.

Gopsill, J. and Jennings, S., 2020. Democratising design through surrogate model convolutional neural networks of computer aided design repositories. Proceedings of the design society: design conference, 1, pp.1285–1294. Available from: https://doi.org/10.1017/dsd.2020.93.

Kittidecha, C. and Marasinghe, A.C., 2015. Application of kansei engineering and box-behnken response surface methodology for shape parameter design: a case study of wine glass. Journal of advanced mechanical design, systems, and manufacturing, 9(5), JAMDSM0059–JAMDSM0059.

Landis, J.R. and Koch, G.G., 1977. The measurement of observer agreement for categorical data. Biometrics, pp.159–174.

Li, L., Jamieson, K., DeSalvo, G., Rostamizadeh, A., and Talwalkar, A., 2017. Hyperband: a novel bandit-based approach to hyperparameter optimization. The journal of machine learning research, 18(1), pp. 6765–6816.

Majoral, X., Becattini, N., O’Hare, J., Bellucci, G., Boujut, J.-F., and Martens, P., 2018. D5.3 demonstration with other creative industries and with customers [Online]. Available from: http://spark-project.net/sites/default/files/file-wp/D5.3_WP5_DEMONSTRATION_WITH_OTHER_CREATIVE_INDUSTRIES_AND_WITH_CUSTOMERS.pdf.

Maturana, D. and Scherer, S., 2015. Voxnet: a 3d convolutional neural network for real-time object recognition. 2015 ieee/rsj international conference on intelligent robots and systems (iros). IEEE, pp.922–928.

Ranscombe, C., Hicks, B., and Mullineux, G., 2012a. A method for exploring similarities and visual references to brand in the appearance of mature mass-market products. Design studies [Online], 33(5), pp.496–520. Available from: https://doi.org/https://doi.org/10.1016/j.destud.2012.04.001.

Ranscombe, C., Hicks, B., Mullineux, G., and Singh, B., 2012b. Visually decomposing vehicle images: exploring the influence of different aesthetic features on consumer perception of brand. Design studies [Online], 33(4), pp.319–341. Available from: https://doi.org/10.1016/j.destud.2011.06.006.

Real, R., Gopsill, J., Jones, D., Snider, C., and Hicks, B., 2021. Distinguishing artefacts: evaluating the saturation point of convolutional neural networks. Cirp design conference. In press.

Venturi, F., Andrich, G., Sanmartin, C., Taglieri, I., Scalabrelli, G., Ferroni, G., and Zinnai, A., 2016. Glass and wine: a good example of the deep relationship between drinkware and beverage. Journal of wine research, 27(2), pp.153–171.

Zaki, H.F., Shafait, F., and Mian, A., 2016. Modeling 2d appearance evolution for 3d object categorization. 2016 international conference on digital image computing: techniques and applications (dicta). IEEE, pp.1–8.



https://doi.org/10.1017/pds.2021.59 Published online by Cambridge University Press